Spring 2-27-2023

On Refinements to QMFD Based Chirp Parameter Estimation

Balu Santhanam
bsanthan@unm.edu

Thalanayar Santhanam

On Refinements to QMFD Based Chirp Parameter Estimation

Balu Santhanam, Department of ECE
University of New Mexico, Albuquerque, NM: 87131
Email: bsanthan@unm.edu

&

Thalanayar S. Santhanam, Emeritus Professor,
Department of Physics, Saint Louis University,
Saint Louis, Missouri 63021.

***Abstract*— Commuting matrix methods furnish a full basis of orthogonal eigenvectors for the discrete Fourier transform or its centered version needed for computing the discrete fractional Fourier transform and multicomponent chirp signal analysis. However, these approaches suffer from ill-conditioning issues at higher matrix sizes, and require a computationally expensive eigenvalue decomposition.**

In this paper, ill-conditioning issues associated with the QMFD approach developed previously by the authors are addressed via diagonal modification. Further symmetries of the eigenvectors are used to reduce the size of the underlying eigenvalue problem. These modifications are then incorporated into the real-arithmetic implementation of the QMFD approach that is shown to be significantly superior to the conventional implementation and the corresponding MSE of the chirp parameter estimates are shown to approach their Cramer Rao lower bounds.

I. Introduction

Chirp signals are quite ubiquitous in various areas of applications in radar and sonar [2] and have recently gained popularity with the LIGO project [3] where gravitational signals from the merger of two black holes are modeled as chirps. Estimating the parameters of the underlying chirp signal model is therefore a problem of significant interest. One such popular tool for multicomponent chirp signal analysis is the DFRFT [5].

The *discrete fractional Fourier Transform* (DFRFT) of a sequence defined as the fractional power of the DFT matrix, formally requires an eigenvalue decomposition [4]

$$\mathbf{X}_\alpha = \mathbf{W}^{\frac{2\alpha}{\pi}}\mathbf{x} = \mathbf{V}\mathbf{\Lambda}\mathbf{V}^T\mathbf{x}, \tag{1}$$

where $\mathbf{W}$ is the DFT matrix, $\mathbf{V}$ is the orthogonal matrix of DFT eigenvectors and $\mathbf{\Lambda}$ is the diagonal matrix of eigenvalues. Commuting matrix approaches towards furnishing a fully orthogonal basis of DFT/CDFT eigenvectors seek to remove the eigenvalue degeneracy inherent in the DFT: [8], [7], [6]

$$\mathbf{T}_c = \mathbf{V}_c\mathbf{\Lambda}_c\mathbf{V}_c^T,$$

where $\mathbf{V}_c$ is the fully orthogonal basis of DFT/CDFT eigenvectors that serve as discrete versions of the Gauss-Hermite functions. In the case of the QMFD approach, the commuting matrix $\mathbf{T}_c$ is obtained via:

$$\mathbf{T}_c = \mathbf{P}^H\mathbf{P} + \mathbf{Q}^H\mathbf{Q}, \quad \mathbf{P} = \mathbf{W}\mathbf{Q}\mathbf{W}^H, \tag{2}$$

where $\mathbf{P}$ and $\mathbf{Q}$ are the finite dimensional equivalents of the position and momentum operators in continuous quantum mechanics, and $\mathbf{W}$ is the CDFT/DFT matrix [6]. Computation of the eigenvectors $\mathbf{V}_c$, requires an eigenvalue decomposition, has significant computational complexity, and becomes a major bottleneck for larger matrix sizes.

These orthogonal eigenvectors are then used to compute the multiangle CDFRFT (MA-CDFRFT) [5]:

$$X_r[k] = \sum_{p=0}^{N-1} z_k[p]e^{-\frac{2\pi}{N}pr}, \tag{3}$$

where the sequence $z_k[p]$ is given by:

$$z_k[p] = v_{kp}\sum_{n=0}^{N-1} x[n]v_{np}$$

and $\{V_c\}_{kp} = v_{kp}$ are derived from the eigenvectors. A monocomponent chirp signal of the form:

$$x[n] = A\cos\left(\omega_o n + c_r m^2\right) + w[n], \quad m = n - (N-1)/2$$

with a specified center-frequency ω_o and chirp-rate c_r, and $w[n]$ is additive white Gaussian noise that is statistically independent of the chirp, manifests as a sharp peak in the MA-CDFRFT spectrum $X_r[k]$ at coordinates (k_p, r_p) that are related to the chirp parameters via [11]:

$$\begin{aligned} \hat{\omega}_o &= -\frac{\pi}{N}\cot\left(\frac{2\pi}{N}r_p - \frac{\pi}{N}\right) \\ \hat{c}_r &= \left(\frac{2\pi}{N}k_p - \frac{\pi}{N}\right)\csc\left(\frac{2\pi}{N}r_p - \frac{\pi}{N}\right). \end{aligned} \tag{4}$$

The corresponding CRLB for the chirp parameter estimates are [12]:

$$\begin{aligned} \sigma^2_{\hat{\omega}_o} &\geq \left(\frac{\sigma}{A}\right)^2 \frac{90}{N(N^2-1)(N^2-4)} \\ \sigma^2_{\hat{c}_r} &\geq \left(\frac{\sigma}{A}\right)^2 \frac{6}{N(N^2-1)}, \end{aligned} \tag{5}$$

where σ^2 is the variance of the zero mean AWGN sequence $w[n]$.

As evident, at its foundation, the QMFD approach relies upon the computation of a fully orthogonal basis of CDFT/DFT eigenvectors for chirp parameter estimation. However, for large matrix orders this approach and other commuting matrix approaches encounter ill-conditioning issues causing problems in eigenvalue decomposition. Furthermore as the matrix size increases the complexity of the approach increases significantly.

In this paper, we introduce refinements to the QMFD approach towards chirp parameter estimation approach by:

1) diagonal modification to address the ill-conditioning problems encountered by the QMFD approach at large matrix orders,
2) incorporating symmetry and anti-symmetry of the eigenvectors are also used to reduce the complexity of computing the needed eigenvectors
3) exploiting symmetries in the commuting matrix to develop a real-arithmetic implementation.

These refinements are further applied to the QMFD chirp parameter estimation technique to: (a) compare the real-arithmetic version with the standard implementation of the commuting matrix approach, and (b) compare the performance of the refined QMFD approach with the Grunbaum approach in terms of the associated MSE.

II. QMFD Refinements

A. Improved Matrix Conditioning

As shown in Fig. (1), the condition number of the commuting matrix associated with the Grunbaum method [7], [9], the QMFD approach [6], and the S matrix [8] approach increases and all three approaches suffer from bad conditioning at larger matrix orders. This specifically causes a loss of orthogonality in the eigenvectors obtained from the MATLAB `eig.m` function.

The conditioning of the matrices can be improved by simply adding a multiple of identity to the commuting matrix. While this modifies the eigenvalues of the commuting matrices, this does not affect the underlying eigenvectors since the underlying commuting matrices are symmetric:

$$\mathbf{T}_{\text{new}} = \mathbf{T}_{\text{old}} + c\mathbf{I} = \mathbf{V}\left(\Lambda + c\mathbf{I}\right)\mathbf{V}^T \tag{6}$$

The condition number of the diagonally modified matrix is given by:

$$\eta_n = \frac{\lambda_{\max} + c}{\lambda_{\min} + c} = \frac{\eta_{\text{o}} + c}{1 + c}, \tag{7}$$

where η_n is the desired condition number and η_o is the old condition number. Other approaches such as rescaling and permutations for improving matrix conditioning with the objective of solving a linear system of equations embodied in the MATLAB function `equilibrate.m` will affect the underlying the underlying eigenvectors. Since the objective of the commuting matrix approach is the orthogonal set of CDFT/DFT eigenvectors, we will not take this approach and instead use the diagonal modification approach.

B. Reduction of the Eigenvalue Problem

The CDFT eigenvectors are solutions to the eigenvalue problem:

$$\mathbf{T}_c\mathbf{V}_c = \Lambda_c\mathbf{V}_c,$$

where $\mathbf{T}_c$ is the commuting matrix that is devoid of eigenvalue degeneracy and $\mathbf{V}_c$ is the matrix of CDFT eigenvectors, whose columns resemble discrete versions of Gauss-Hermite functions. In the case of the Grunbaum commuting matrix, $\mathbf{T}_c$ is a symmetric tridiagonal matrix, while for the QMFD approach the commuting matrix is a full symmetric matrix. In both these cases, the matrix of eigenvectors has even and odd symmetry.

Consequently the eigenvalue problem can be reduced to a smaller eigenvalue problem for the even and odd eigenvectors. Upon incorporating the symmetry and anti-symmetry into the matrix of eigenvectors we obtain the reduced eigenvector systems as described in [10]:

$$\begin{aligned} \left(\mathbf{T}_a + \mathbf{T}_b\right)\mathbf{V}_e &= \Lambda_e\mathbf{V}_e \\ \left(\mathbf{T}_a - \mathbf{T}_b\right)\mathbf{V}_o &= \Lambda_o\mathbf{V}_o, \end{aligned} \tag{8}$$

where $\mathbf{V}_e$ is the matrix containing half of the symmetric eigenvectors and $\mathbf{V}_o$ is the matrix containing half of the skew-symmetric eigenvectors. The matrices $\mathbf{T}_a$ and $\mathbf{T}_b$ are given by:

$$\mathbf{T}_a = \begin{pmatrix} T(1,1) & T(1,2) & \dots & T(1,\frac{N}{2}) \\ T(2,1) & T(2,2) & \dots & T(2,\frac{N}{2}) \\ \vdots & \vdots & \dots & \vdots \\ T(\frac{N}{2},1) & T(\frac{N}{2},2) & \dots & T(\frac{N}{2},\frac{N}{2}) \end{pmatrix}$$

and

$$\mathbf{T}_b = \begin{pmatrix} T(1,N) & T(1,N-1) & \dots & T(1,\frac{N}{2}+1) \\ T(2,N) & T(2,N-1) & \dots & T(2,\frac{N}{2}+1) \\ \vdots & \vdots & \dots & \vdots \\ T(\frac{N}{2},N) & T(\frac{N}{2},N-1) & \dots & T(\frac{N}{2},\frac{N}{2}+1) \end{pmatrix}$$

These matrices can in turn be expressed in terms of the exchange matrix as [10]:

$$\begin{aligned} \mathbf{T}_e &= \mathbf{T}_a + \mathbf{T}_b = \mathbf{T}_a + \mathbf{T}_c\mathbf{J}, \\ \mathbf{T}_o &= \mathbf{T}_a - \mathbf{T}_b = \mathbf{T}_a - \mathbf{T}_c\mathbf{J}, \end{aligned} \tag{9}$$

where $\mathbf{T}_c$ is the principal minor:

$$\mathbf{T}_c = \begin{pmatrix} T(1,\frac{N}{2}+1) & T(1,\frac{N}{2}+2) & \dots & T(1,N) \\ T(2,\frac{N}{2}+1) & T(2,\frac{N}{2}+2) & \dots & T(2,N) \\ \vdots & \vdots & \dots & \vdots \\ T(\frac{N}{2},\frac{N}{2}+1) & T(\frac{N}{2},\frac{N}{2}+2) & \dots & T(\frac{N}{2},N) \end{pmatrix},$$

and $\mathbf{J}$ is the exchange matrix with the same dimension as these matrices, Both of these matrices $\mathbf{T}_a$ and $\mathbf{T}_c$ are principal minor matrices of $\mathbf{T}$, are of dimension $\frac{N}{2} \times \frac{N}{2}$, so the effective eigenvalue problem has been reduced to 2 smaller eigenvalue problems. Once $\mathbf{V}_e$ and $\mathbf{V}_o$ are extracted from Eq. (8), $\mathbf{V}_c$ can be constructed from even and odd symmetry.

C. Real-Arithmetic Implementation

The standard QMFD commuting matrix has elements defined via the almost Toeplitz operator[13]:

$$T_{rs}^{(1)} = \begin{cases} \dfrac{4\pi}{N^2}\displaystyle\sum_{l=0}^{N-1}(l-m)^2 + \dfrac{2\pi}{N}(r-m)^2 & r = s \\ \dfrac{4\pi}{N^2}\displaystyle\sum_{l=0}^{N-1}(l-m)^2 W_N^{(l-m)(r-s)} & r \neq s, \end{cases} \tag{10}$$

where $m = (N-1)/2$. In our implementations N is even and specifically $N = 2^\nu$, since we employ radix-2 FFT algorithms [1]. The quadratic factors in the above expression are symmetric about the midpoint: $l = m$. This means that the sums in the above expression can be simplified further to yield:

$$T_{rs}^{(2)} = \begin{cases} \dfrac{4\pi}{N^2}\displaystyle\sum_{l=0.5}^{m}(l-m)^2 + \dfrac{2\pi}{N}(r-m)^2 & r = s \\ \dfrac{4\pi}{N^2}\displaystyle\sum_{l=0.5}^{m}(l-m)^2\cos(2\pi(l-m)(r-s)/N) & r \neq s, \end{cases} \tag{11}$$

These expressions are equivalent from a infinite precision arithmetic viewpoint, the primary difference between the two expressions is that the original QMFD commuting matrix is defined via N-point sums, while the real-arithmetic version only has $\frac{N}{2}$-point sums, resulting in lesser round-off error. As we will see, the resulting chirp parameter estimates will have significantly different performances from a MSE point of view.

If we further incorporate windowing of the diagonal position operator $\mathbf{Q}$ with Kaiser windowing [13]:

$$T_{rs}^{(2)} = \begin{cases} \dfrac{4\pi}{N^2}\displaystyle\sum_{l=0.5}^{m}(l-m)^2 w^2[l] + \dfrac{2\pi}{N}(r-m)^2 w^2[r], & r = s \\ \dfrac{4\pi}{N^2}\displaystyle\sum_{l=0.5}^{m}(l-m)^2\cos(\dfrac{2\pi}{N}(l-m)(r-s))w^2[l], & r \neq s, \end{cases} \tag{12}$$

where $w[r]$ is the window used to mitigate truncation effects.

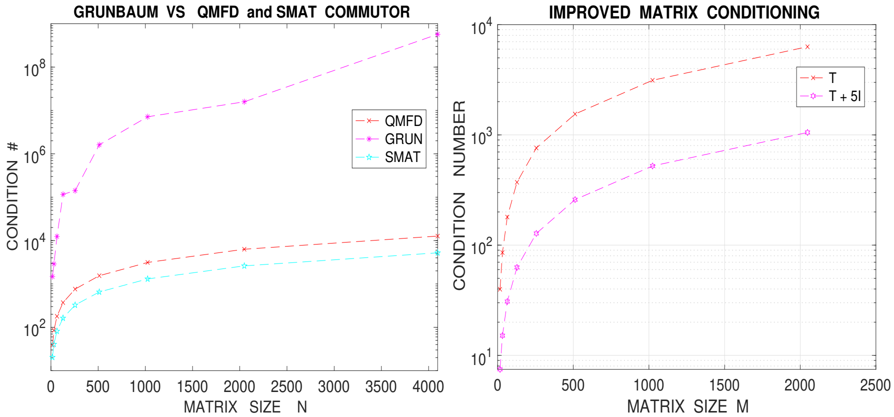

(a) (b)

Fig. 1. Improved matrix conditioning: (a) Condition numbers for various CDFT commuting matrix approaches and (b) condition numbers before and after diagonal modification with $c = 5$, depicting a significant decrease in condition number.

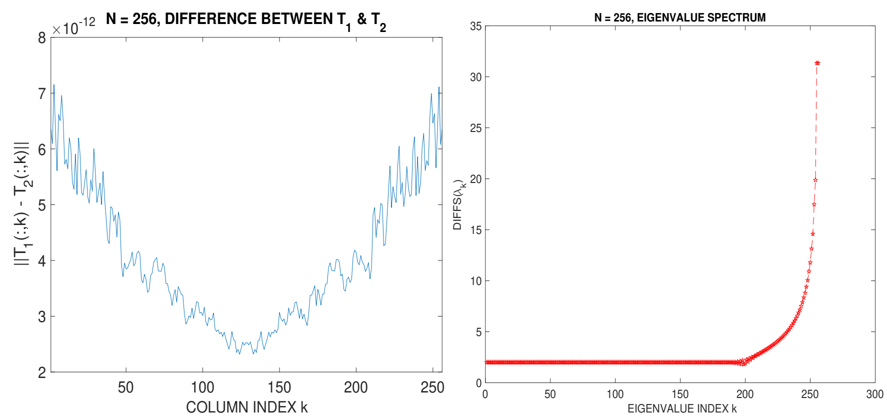

(a) (b)

Fig. 2. Difference between $\mathbf{T}_1$ and $\mathbf{T}_2$: (a) norm of the difference between columns of $\mathbf{T}_1$ and $\mathbf{T}_2$ and (b) symmetric difference of. the eigenvalue spectrum of $\mathbf{T}_2$. These clearly depict the equivalence between the two matrices.

Fig. (2)(a) depicts the norm of the difference between the columns of the two versions of the QMFD commuting matrix and Fig. (2)(b) depicts the symmetric difference of the eigenvalue spectrum of the matrix $\mathbf{T}_2$ confirming that they are indeed the same apart from numerical precision differences.

Fig. (3)(a,b) depict the MSE of the center-frequency and chirp-rate estimators of both the original and the real-arithmetic implementation of the QMFD commuting matrix for $N = 128$ and $M = 256$ averaged over 2400 experiments. Fig. (3)(c,d) depict the MSE of the parameter estimates for $N = 128$ and $M = 512$. These results clearly indicate a significant improvement of about 20 dB for the center-frequency estimates and 40 dB for the chirp-rate estimates in terms of the MSE between the original QMFD and its real-arithmetic implementation for the former setting and about a 25 dB improvement for both parameter estimates in the latter setting. Henceforth in this paper, we will use the real-arithmetic QMFD implementation.

III. Discussion

Upon incorporating diagonal modification with $c = 5$, the eigenvalue reduction technique into the real-arithmetic implementation of the QMFD approach to chirp parameter estimation, we can now study its performance for large matrix orders M, where M is the duration of the signal after zero-padding symmetrically on both sides. We specifically apply the refined approach for $M = 4096$ and 8192, large values for the matrix size, that would have normally resulted in orthogonality issues in the computed eigenvectors and computational bottlenecks due to the size of the eigenvalue problem.

Fig. (4)(a,b) depict the MSE of the QMFD chirp parameter estimates using the proposed approach for smaller values of M, clearly showing a steady movement of the MSE of the chirp parameter estimates towards the corresponding CRLB values as the matrix size increases. Fig. (4)(c,d) depict the performance of the QMFD approach for larger matrix sizes using the approach presented here. Simulation results depict a clear and steady movement of the MSE of the QMFD chirp parameter estimates towards the CRLB for both estimators and a clear improvement in the MSE performance at lower SNR's with increased zero-padding length M.

Figure (5) depicts the performance of the Grunbaum commuting matrix approach chirp parameter estimates for $M = 2048$, $M = 4096$, and $M = 8192$ using the refinements presented in this work averaged over 2000 experiments. Simulation results depict a similar movement of the MSE of the parameter estimates towards the CRLB, as observed with the refined QMFD approach, with improvement at lower SNR values and a slight increase in the MSE at higher SNR values, with increase in M, for both parameter estimates. For the same chirp parameter set, it can be seen that the QMFD approach produces smaller MSE's, at larger matrix sizes in comparison to the

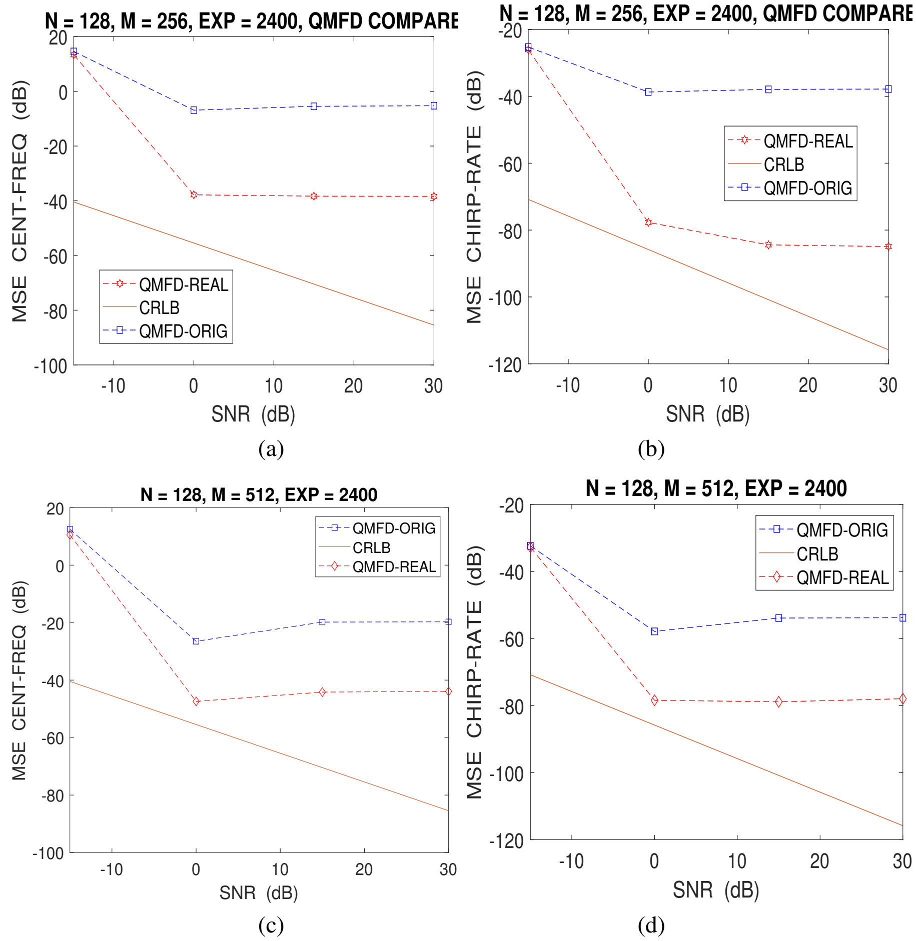

Fig. 3. Comparison between QMFD implementations: (a,b) MSE of center-frequency estimators in relation to the CRLB and (b) MSE of the chirp-rate estimators for $N = 128$ and $M = 256$ in relation to the CRLB, (c,d) MSE of estimators for $N = 128$ and $M = 512$.

Grunbaum approach.

IV. Conclusions

In this paper, we have presented several refinements to the basic QMFD approach towards chirp parameter estimation intended to address commuting matrix ill-conditioning issues and computational complexity issues associated with eigenvalue decomposition for large matrix orders. These refinements were incorporated into the QMFD approach and used to show that the MSE performance of the QMFD real-arithmetic version is significantly superior to that obtained via the standard QMFD implementation. It was also shown that with the aid of these refinements, the MSE's of the QMFD chirp parameter estimates approach the corresponding CRLBs for larger matrix orders.

References

[1] A. V. Oppenheim and R. W. Schafer, “Discrete-time Signal Processing,” Third Edition, Pearson Publishing Company, 2009.

[2] R. M. Liang and K. S. Arun, “Parameter Estimation of Superposition of Chirp Signals,” *Proceedings of IASSP 1992*, pp. 273-276, March 1992.

[3] ”Gravitational Wave Spectrogram,” Laser Interferometer Gravitational Wave Observatory (LIGO), website: `ligo.caltech.edu`, California Institute of Technology, 2017.

[4] Balu Santhanam and J. H. McClellan, “The Discrete Rotational Fourier Transform,” *IEEE Transactions om Signal Processing*, Vol. 44, No. 4, pp. 994-998, April, 1996.

[5] J. G. Vargas-Rubio and Balu Santhanam, “On the Multiangle Centered Discrete Fractional Fourier Transfom,” *IEEE Signal Processing Letters*, Vol. 12, No. 4, pp. 273-276, 2005.

[6] Balu Santhanam and T. S. Santhanam, “On Discrete Gauss-Hermite Functions and Eigenvectors of the Discrete Fourier Transform,” *Signal Processing*, Vol. 88, No. 11, pp. 2738-2746, 2008.

[7] F. A. Grunbaum, “The Eigenvectors of the Discrete Fourier Transform: A Version of the Hermite Functions,” *Journal of Mathematical Analysis and Applications*, Vol. 88, pp. 355-363, 1982.

[8] B. W. Dickinson and K. Steiglitz, “Eigenvectors and Eigenfunctions of the Discrete Fourier Transform,” *IEEE Transactions on Signal Processing*, Vol. 30, No. 1, pp. 25-31, 1982.

[9] S. Clary and D. H. Mugler, “Shifted Fourier Matrices and their Tridiagonal Commutors,” *SIAM Journal on Matrix Analysis and Applications*, Vol. 24, No. 3, pp. 809-821, 2003.

[10] A. Cantoni and P. Butler, “Eigenvalues and Eigenvectors of Symmetric Centrosymmetric Matrices,” *Linear Algebra and Its Applications*, Vol. 13, No. 3, pp. 275-288, April 1976.

[11] S. Mandal, Balu Santhanam, and M. Hayat, “On Improved Accuracy Chirp Parameter Estimation Using The DFRFT with Application to SAR-Based Vibrometry,” *Proc. of Ailomar 2018*, pp. 1098-1102, 2018.

[12] D. J. Peacock and B. Santhanam, “Multicomponent Subspace Chirp Parameter Estimation Using Discrete Fractional Fourier Analysis,” url: `https://www.osti.gov/biblio/1106703`, Sep., 2011.

[13] Balu Santhanam, Thalanayar Santhanam, and Satish Mandal, “On the Effects of Windowing on the Discretization of the fractional Fourier Transform,” *Proc. of Asilomar 17*, pp. 233 - 237, 2017.

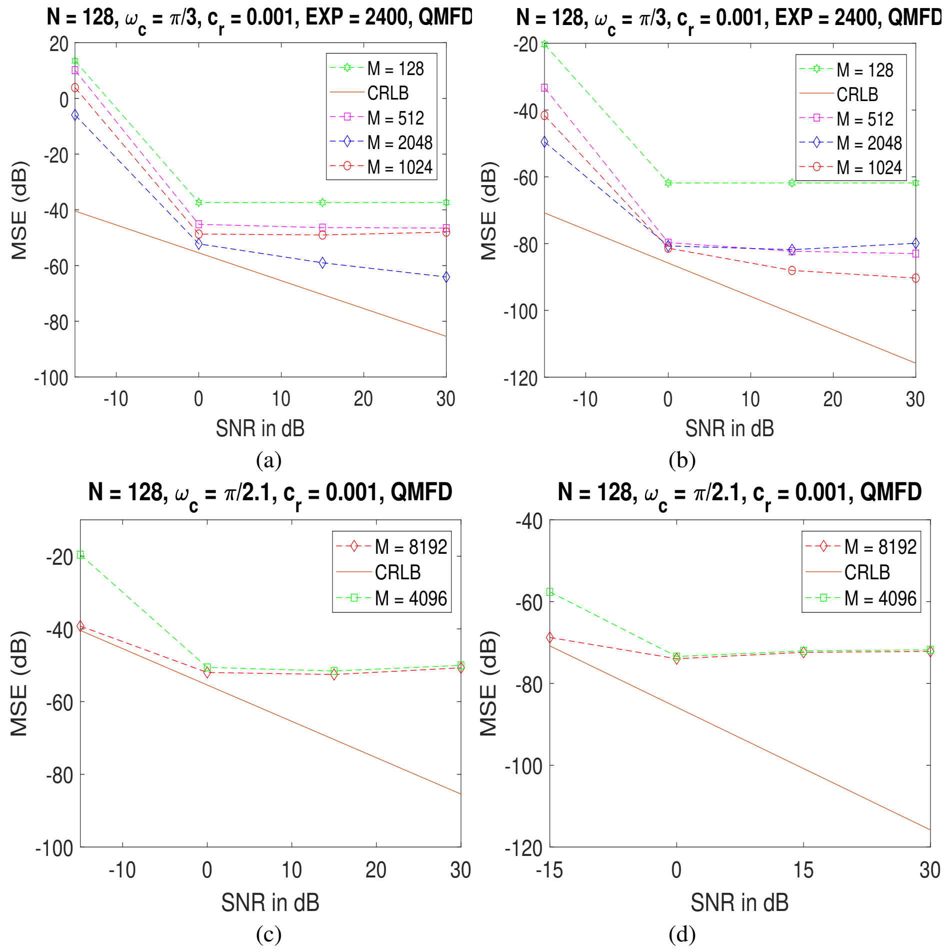

Fig. 4. MSE performance of the QMFD center-frequency and chirp-rate estimators versus CRLB for: (a,b) $M = 128, 512, 1024, 2048$ (averaging over 2400 experiments) and (c,d) $M = 4096, 8192$ (averaging over 300 experiments), using $c = 5$ for the diagonal modification and eigenvalue problem reduction.

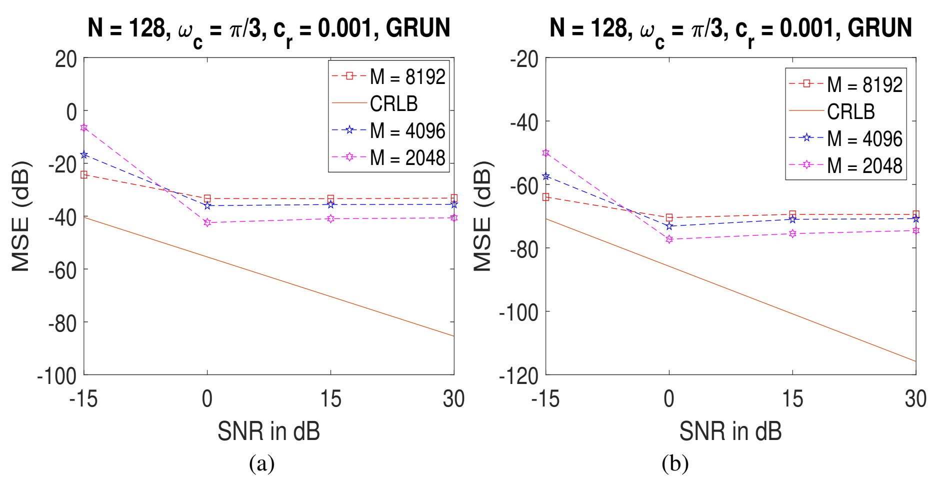

Fig. 5. Comparison of the MSE performance of the chirp parameter estimates of the Grunbaum approach for $M = 2048, 4096, 8912$ with $c = 5$, in comparison to the CRLB, obtained by averaging over 2000 experiments.